

THE FORMATION OF THE FIRST QUASARS IN THE UNIVERSE

JOSEPH SMIDT¹, DANIEL J. WHALEN², JARRETT L. JOHNSON¹ AND HUI LI¹*Draft version March 3, 2017*

ABSTRACT

Supermassive black holes are the central engines of luminous quasars and are found in most massive galaxies today. But the recent discoveries of ULAS J1120+0641, a $2 \times 10^9 M_\odot$ black hole at $z \sim 7.1$, and SDSS J0100+2802, a $1.2 \times 10^{10} M_\odot$ black hole at $z = 6.3$, challenge current paradigms of cosmic structure formation because it is not known how quasars this massive appeared less than a billion years after the Big Bang. Here, we report new cosmological simulations of SMBHs with x-rays fully coupled to primordial chemistry and hydrodynamics that show that J1120+0641 and J0100+2802 can form from direct collapse black holes if their growth is fed by cold, dense accretion streams, like those thought to fuel the rapid growth of some galaxies at later epochs. Our models reproduce the mass, luminosity and ionized near zone of J1120+0641, as well as the star formation rate and metallicity in its host galaxy. They also match new observations of the dynamical mass of the central 1.5 kpc of its emission region just obtained with ALMA. We find that supernova feedback from star formation in the host galaxy regulates the growth of the quasar from early times.

Subject headings: quasars: supermassive black holes — black hole physics — early universe — dark ages, reionization, first stars — galaxies: formation — galaxies: high-redshift

1. INTRODUCTION

Over 100 quasars have now been found at $z > 6$, including ULAS J1120+0641, a $2 \times 10^9 M_\odot$ black hole at $z \sim 7.1$, and SDSS J0100+2802, a $1.2 \times 10^{10} M_\odot$ black hole at $z = 6.3$ (Mortlock et al. 2011; Wu et al. 2015). Their discovery poses severe challenges to current theories of cosmic structure formation because it is not known how quasars this massive formed by such early times. But there is now reason to doubt that Population III (Pop III) stars at $z \sim 25$ were not the origin of supermassive black holes (SMBHs) at $z \gtrsim 7$ because they would have had to accrete continuously at nearly the Eddington limit after collapse to reach $10^9 M_\odot$ in just 500 Myr. This scenario is not likely for several reasons.

First, ionizing UV flux from primordial stars generally evicts all the baryons from their host halos, so they collapse to BHs in low-density H II regions that prevent rapid initial accretion (e.g. Kitayama et al. 2004; Whalen et al. 2004). X-rays from the BH later evaporate cosmological flows from the halo until it reaches masses with escape velocities that are greater than the sound speed in the ionized gas (Alvarez et al. 2009; Park & Ricotti 2011). This may be true even of super-Eddington accretion scenarios often invoked as solutions to the rapid growth problem with Pop III star BHs (Volonteri et al. 2015; Sakurai et al. 2016; Pezzulli et al. 2016). Low-mass Pop III star BHs are also prone to natal kicks that can eject them from their host halos, and thus their fuel supply (Whalen & Fryer 2012).

For these reasons, it is now suspected that direct collapse black holes (DCBHs) may have instead been the seeds of the first quasars (see e.g. Johnson et al. 2013). They form when catastrophic baryon collapse triggered by atomic cooling in pristine $10^8 M_\odot$ halos at $z \sim 20$

pools gas at their centers at rates of $0.1 - 10 M_\odot \text{ yr}^{-1}$ (Wise et al. 2008; Regan & Haehnelt 2009; Shang et al. 2010; Latif et al. 2013; Becerra et al. 2015). A supermassive star or quasi-star forms and later collapses to a $\sim 10^5 M_\odot$ BH. Halos reaching this mass without having previously formed stars via H_2 cooling must be in close proximity to strong sources of Lyman-Werner (LW) UV photons (e.g., Agarwal et al. 2012; Dijkstra et al. 2014), be collisionally ionized by strong accretion shocks (Inayoshi & Omukai 2012), or be collisionally dissociated by a recent, violent merger (Inayoshi et al. 2015). Although they form at later times, DCBHs can grow at much higher rates than Pop III star BHs because they are born with much larger masses and in much higher densities in host galaxies that can retain their fuel supply even, when it is heated by x-rays (e.g. Pacucci et al. 2015). One may now have been discovered in the Ly- α emitter CR7 at $z = 6.6$ (e.g. Sobral et al. 2015; Hartwig et al. 2016; Smith et al. 2016; Agarwal et al. 2016; Whalen et al. 2017).

But to exceed $10^9 M_\odot$ by $z \sim 7$, a DCBH must also form in a halo fed by unusually strong cold accretion flows, like those thought to fuel the rapid growth of some galaxies at later epochs (e.g., Dekel et al. 2009). There may be up to a few dozen regions per Gpc^{-3} with cold flows capable of forming quasars at $z \gtrsim 7$ (Di Matteo et al. 2012; Feng et al. 2014) (see also Costa et al. 2014; Hirschmann et al. 2014). Unfortunately, these studies could not resolve the flows deep in the host galaxy at early times. Other models that have resolved them did so at lower redshifts and were decoupled from accretion flows on cosmological scales (e.g., Bournaud et al. 2011). Aykutaalp et al. (2014) examined X-ray breakout from a DCBH in an atomically cooling halo, but not in cold flows and only for short times to estimate early growth rates. Until now, no single simulation has connected quasar growth on both scales from initial formation down the end of reionization with X-rays from the BH, which de-

¹ Los Alamos National Laboratory, Los Alamos, NM 87545² Institute of Cosmology and Gravitation, Portsmouth University, Dennis Sciamia Building, Portsmouth PO1 3FX, UK

grade or destroy cold streams in the host halo and in the early intergalactic medium (IGM).

We have now developed numerical models that bridge both scales and evolved a quasar from birth at $z \sim 20$ down to $z \sim 6$ in cold flows with x-rays from the BH fully coupled to primordial gas chemistry and hydrodynamics. We describe our numerical model in Section 2 and the evolution of the BH and its host galaxy in Section 3. We discuss prospects for the detection of the first quasars and conclude in Section 4.

2. NUMERICAL METHOD

We use the Enzo adaptive mesh refinement (AMR) cosmology code (Bryan et al. 2014), which evolves dark matter with an adaptive N -body particle-mesh scheme and gas flows with a piecewise-parabolic method. X-rays from the BH are transported with the MORAY photon-conserving adaptive raytracing radiation package (Wise & Abel 2011), which is self-consistently coupled to hydrodynamics and nine-species primordial gas chemistry in Enzo and includes radiation pressure on gas due to photoionizations. Our simulation has a uniform LW UV background due to global Pop III and Pop II SF that evolves with redshift.

Secondary ionizations by energetic photoelectrons and Compton heating by x-rays are included in the chemistry and cooling, and we assume a single photon energy of 1 keV. In reality, there is a spectrum of energies that evolves from X-rays to hard UV as the black hole grows four decades in mass, but we chose 1 keV to maximize heating and evaporation because photons with higher energies have much lower ionization cross sections. Our models therefore produce an upper limit to radiative feedback by the BH. The BH is represented by a modified star particle that grows in mass as it accretes gas. Its luminosity, L_r , is $\epsilon_r \dot{m}_{BH} c^2$, where ϵ_r is the mean radiative efficiency, which we take to be 0.1, and \dot{m}_{BH} is the accretion rate. To approximate mechanical feedback by a BH jet, $10^{-4} L_r$ is deposited as thermal energy above and below the midplane of the BH perpendicular to its angular momentum vector (Ciotti et al. 2009).

Our simulation box is $100 h^{-1}$ Mpc on a side, with a 256^3 root grid and three nested $25 h^{-1}$ Mpc grids that are centered on the host halo for an effective resolution of 2048^3 . These grids yield initial dark matter and baryon mass resolutions of $8.41 \times 10^6 h^{-1} M_\odot$ and $1.57 \times 10^6 h^{-1} M_\odot$, respectively. The grid is initialized with gaussian primordial density fluctuations at $z = 200$ with MUSIC (Hahn & Abel 2011) with cosmological parameters from the second-year *Planck* best fit lowP+lensing+BAO+JLA+ H_0 : $\Omega_M = 0.308$, $\Omega_\Lambda = 0.691$, $\Omega_b = 0.0223$, $h = 0.677$, $\sigma_8 = 0.816$, and $n = 0.968$ (Planck Collaboration et al. 2016). We use a maximum refinement level $l = 10$ and refine the grid on baryon overdensities of $3 \times 2^{-0.2l}$ to obtain a maximum resolution of 35 pc. We also refine on a dark matter overdensity of 3 and resolve the local Jeans length with at least 32 zones at all times to avoid artificial fragmentation during collapse.

Our simulation box was chosen to be large enough to enclose the cold flows feeding the quasar on cosmological scales while resolving gas flows, photoionization and SF deep within its host galaxy. However, given that there are only about a dozen regions per Gpc^{-3} with cold flows

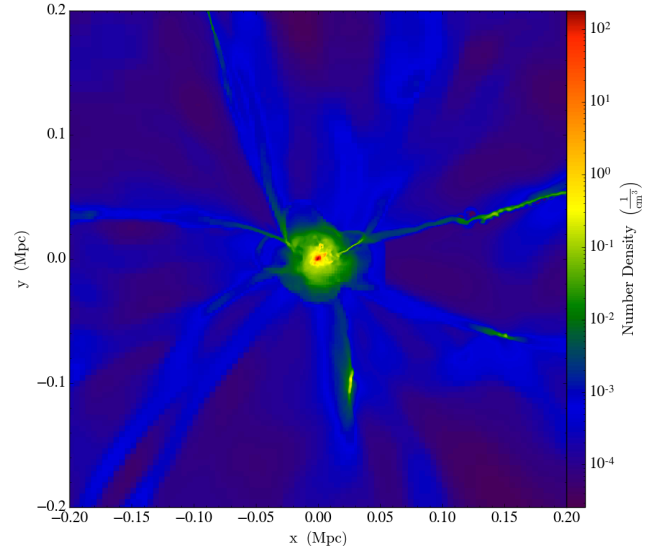


FIG. 1.— Density slice of the host halo of the quasar at $z = 7.1$. Cold accretion streams intersecting the host galaxy of the quasar are clearly visible. Distances are in comoving Mpc.

capable of sustaining rapid quasar growth, no single 100 Mpc box at random would be expected to enclose one. We therefore tested multiple random seeds at lower resolution until we obtained a halo that exceeded $10^{12} M_\odot$ by $z \sim 7$ and was not the product of major mergers, i.e., no mergers with other halos similar in mass to the host halo at any redshift prior to $z \sim 7$ (Trenti et al. 2008). The host halo of the BH is shown at $z = 7.1$ in Fig. 1, when the cold flows are most prominent.

Our simulations do not resolve the accretion disk of the BH, which is 0.1 - 1 pc in diameter. We therefore use an alpha disk model to compute accretion rates instead of the usual Bondi-Hoyle rates to approximate angular momentum transport out of the disk on subgrid scales (DeBuhr et al. 2010). Molecular clouds are not resolved in our runs either, so we use a stochastic prescription for SF (section 8.2.2 of Bryan et al. 2014) that is based on Cen & Ostriker (1992). The stars are assumed to have a Salpeter initial mass function (IMF) for simplicity. Feedback by supernovae (SNe) is represented as thermal energy deposited in the SF regions with 10^{51} erg deposited per explosion, assuming about one SN per 200 M_\odot of stars formed. Cooling by metals from SNe is included with rates from Glover & Jappsen (2007) and Sutherland & Dopita (1993), assuming solar yields for the ejecta that are consistent with our chosen IMF.

3. SMBH / HOST GALAXY COEVOLUTION

We first evolve the box from $z = 200$ down to $z = 19.2$, when the host halo reaches $3.0 \times 10^8 M_\odot$ and crosses the mass threshold for atomic cooling and collapse. At this redshift we initialize a $10^5 M_\odot$ BH particle at the center of the halo and turn on x-rays and SF. We omit the formation and collapse of the supermassive star because it occurs on timescales of a few hundred kyr, less than the cosmological time step of the simulation. Stellar evolution models also indicate that the star evolves as a red supergiant whose radiation cannot alter the flows that create it or cold streams entering the halo (e.g. Begelman 2010; Hosokawa et al. 2013; Schleicher et al. 2013;

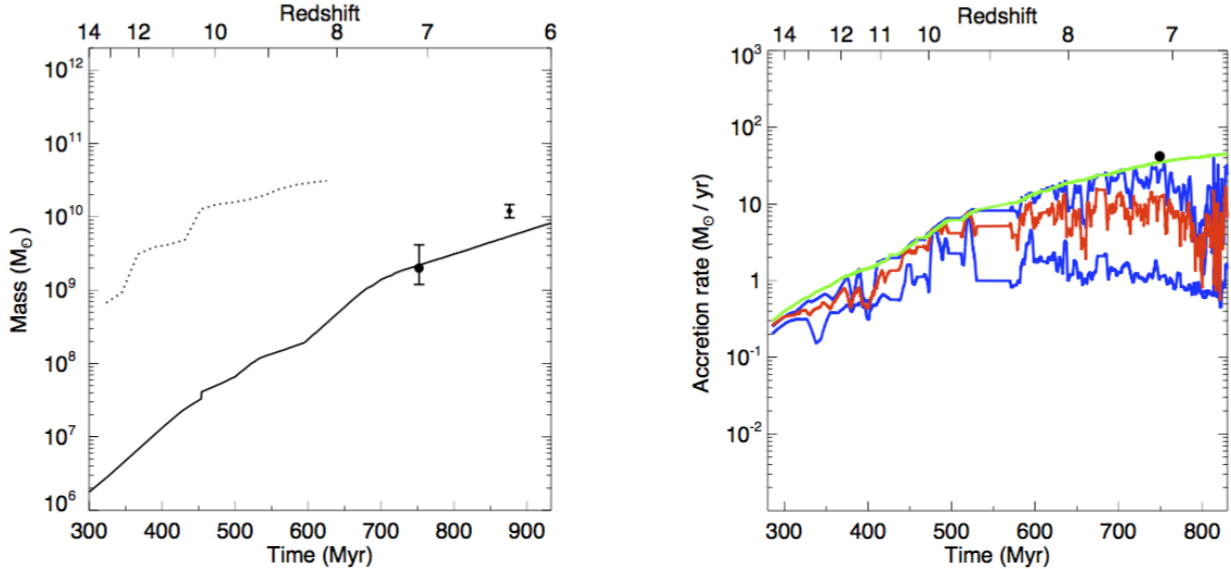


FIG. 2.— Left panel: BH mass (solid line) and halo mass (dotted line) as functions of time and redshift. The solid black circles and their error bars are the masses of J1120+0641 and J010013.02+280225.8 inferred from observations at $z = 7.1$ and 6.3 , respectively. Right panel: average accretion rates (red), upper and lower limits on the accretion rate (blue) and the Eddington rate (green). The black circle is the accretion rate for the observed bolometric luminosity of J1120+0641, assuming $\epsilon = 0.1$.

Sakurai et al. 2016b; Hammerlé et al. 2017). Other studies show that even if the rapidly accreting star becomes a luminous source of ionizing UV radiation, the flux could not overcome the ram pressure of the inflow and break through it (Johnson et al. 2012). Our choice of seed mass is consistent with the most recent simulations that place an upper limit of a few $10^5 M_\odot$ on supermassive stars collapsing via the general relativistic instability in atomically-cooled halos (e.g. Chen et al. 2014; Latif et al. 2013b; Umeda et al. 2016; Becerra et al. 2017; Woods et al. 2017).

BH masses, halo masses and accretion rates are shown in Fig. 2 and SF rates (SFRs) in the host galaxy and average accretion rates normalized to the Eddington limit are shown in Fig. 3. Actual accretion rates vary rapidly between the upper and lower limits shown in red, with average values in blue. Prior to the onset of SF in the host galaxy, X-rays from the nascent BH initially limit average accretion rates to $0.8 \dot{m}_{\text{Edd}}$, where \dot{m}_{Edd} is the Eddington accretion limit, but this fraction soon falls to 0.3 by 100 Myr as the BH grows two decades in mass. But at 400 Myr the host halo merges with another, smaller halo as shown in Fig. 4 and in the jump in halo mass in Fig. 2. The collision triggers a small starburst at 420 Myr as shown in Fig. 3. Disruption of the halo by the merger and SN feedback from the subsequent burst perturb the flows in the vicinity of the BH, inducing the brief surges of super-Eddington accretion at 475 Myr and 510 Myr in Fig. 3. These two processes cause the slight jump in BH mass visible at 450 Myr ($z = 10.7$) in Fig. 2. The accretion ratio again begins to fall as this first starburst subsides.

Fed by cold flows, the halo then rapidly grows from $5 \times 10^9 M_\odot$ at $z \sim 11$ to $1.2 \times 10^{12} M_\odot$ by $z = 7.1$. These flows fuel a much larger starburst that peaks at $770 M_\odot \text{ yr}^{-1}$ at $z = 7.8$. The much stronger SN feedback from this burst and the larger X-ray fluxes from the now more

massive BH cause its average accretion efficiency to fall after 500 Myr, eventually to $0.2 \dot{m}_{\text{Edd}}$ by 900 Myr. Even so, the upper limit to the fluctuations in these rates is still nearly the Eddington limit at $z = 7.1$, consistent with observations of J1120+0641 as shown in Fig. 2. At no time do we artificially cap accretion rates onto the BH; except for brief episodes, x-rays and SN feedback limit them to below the Eddington rate throughout the life of the BH. The second, much larger burst in SF is quenched by its own violent SN feedback, falling to $\sim 150 M_\odot \text{ yr}^{-1}$ by $z \sim 7.3$. The SFR then recovers but levels off, never again exceeding $\sim 300 M_\odot \text{ yr}^{-1}$ because of rising X-ray fluxes from the BH, even though cold streams continue to flow into the halo as shown in Fig. 2.

At $z = 7.1$ the BH mass is $2.15 \times 10^9 M_\odot$, well within the error bars in mass of J1120+0641 at this redshift. The SFR in the host galaxy is $245 M_\odot \text{ yr}^{-1}$, consistent with those observed for J1120+0641 ($60 - 270 M_\odot \text{ yr}^{-1}$; Barnett et al. 2015; Venemans et al. 2017). The dynamical mass of the central 1.5 kpc of the host galaxy is $3.95 \times 10^{10} M_\odot$, in good agreement with new observations of J1120+0641 with the Atacama Large Millimeter Array (ALMA; Venemans et al. 2017). As shown in Fig. 5, metallicities are mildly supersolar ($\sim 2 Z_\odot$) at the center of the host galaxy and approximately solar in the rest of its interior, as found in observations (Fig. 2 in Dunlop 2013). Metals are also visible in nearby halos and in some of the accretion filaments threading the host galaxy. The spherically-averaged temperature profile of the H II region of the quasar at $z = 7.1$ is shown in the right panel of Fig. 5. Both X-rays from the BH and SNe heat gas in the host galaxy to a few 10^6 K and the X-rays heat the surrounding IGM to temperatures of $10^4 - 10^5 \text{ K}$. Temperatures of 10^4 K extend out to $\sim 2 \text{ Mpc}$ from the quasar, which is the observed radius of the ionized near zone of J1120+0641.

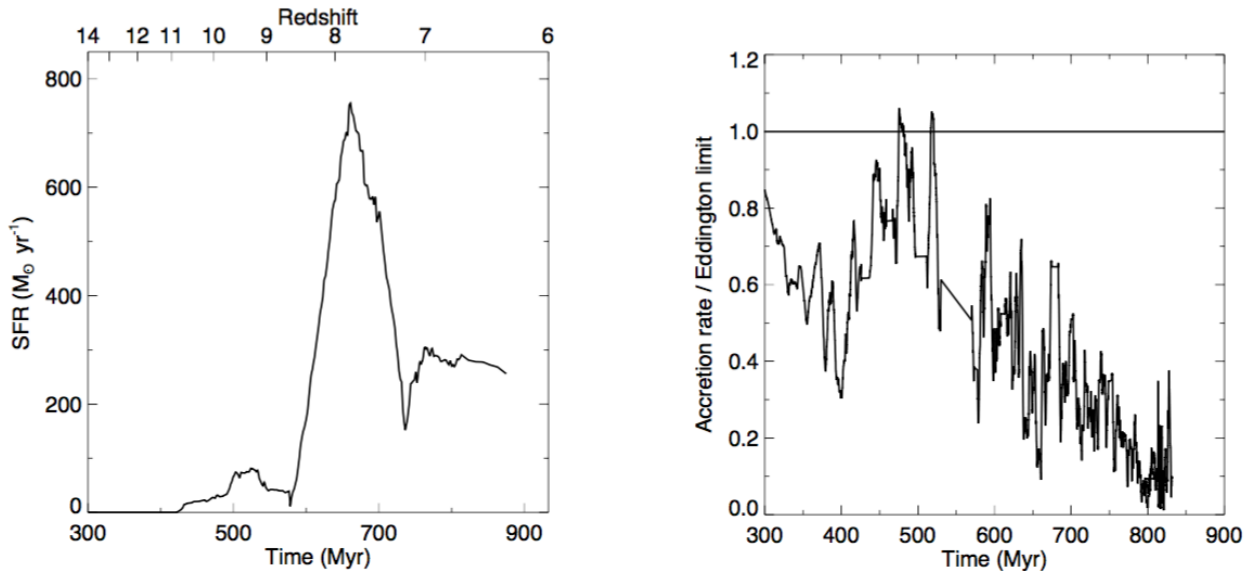


FIG. 3.— Left panel: Star formation rates in the host galaxy of the BH. Right panel: accretion rates normalized to the Eddington limit.

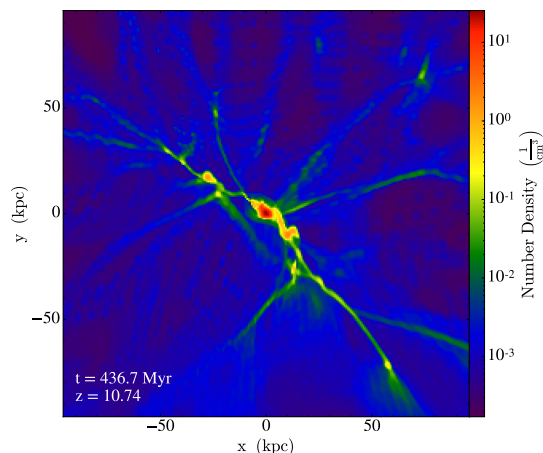


FIG. 4.— Onset of the merger at $z \sim 11$ that triggers the first burst of star formation in the host halo of the BH.

4. DISCUSSION AND CONCLUSION

Our numerical simulations show that the earliest quasar discovered to date, ULAS J1120+0641, can be explained as a DCBH that formed at the intersection of cold accretion streams at $z \sim 20$. They also show how the more massive quasar SDSS J0100+2802 could have formed at slightly lower redshifts. The BH in our model reaches $5.44 \times 10^9 M_\odot$ by $z = 6.3$, within a factor of 2 of the observed one, and well within the uncertainty in mass of a factor of three associated with the use of the Mg II line as a proxy for the luminosity of SDSS J0100+2802.

We note that SF begins at earlier times in Aykutalp et al. (2014) than in our models, triggered by X-rays from the BH that produce energetic photoelectrons that cause secondary ionizations that enhance free electron fractions in the primordial gas. Free electrons catalyze the formation of H_2 via the H^- channel, cooling the gas and forming stars. However, SF only occurred in the central few pc of the halo in their models, well below the reso-

lution limit of our simulations, so the BH would have to grow to larger masses in our models before its X-ray flux could trigger SF at larger radii. However, as discussed in the previous section, the merger at $z \sim 11$ triggers SF before X-rays can. Furthermore, the host halo in the Aykutalp et al. (2014) models was not at the nexus of cold accretion streams, whose turbulent flows may have delayed the onset of SF in their study. Radiation and SN feedback limit accretion rates to at most $0.1 \dot{m}_{\text{Edd}}$ in Aykutalp et al. (2014), but they would be expected to be larger in the higher ram pressures of the cold flows in our models. The delayed onset of SF in our simulations is also in part due to our lower resolution, which cannot capture individual molecular clouds so greater baryonic masses and densities must build up in the halo before the criteria for SF are satisfied.

Although our simulations include a prescription for mechanical feedback from a BH jet, it is not clear if one would actually form at the accretion rates in our models. Steady jets are observed in active galactic nuclei (AGNe) at $L \lesssim 0.01 L_{\text{Edd}}$ and intermittent jets are seen in quasars at $L \sim L_{\text{Edd}}$ (Merloni & Heinz 2008). In these cases the disk is geometrically thick and radiatively inefficient. No jets are seen at $0.01 L_{\text{Edd}} < L < L_{\text{Edd}}$, when the disk is geometrically thin and radiatively efficient. Regardless, when we repeated our simulation without a jet we found little effect on BH mass over time.

Other direct collapse scenarios could produce less massive BH seeds at high redshift. For example, if a $10^8 M_\odot$ halo is marginally enriched by a SN explosion the gas can fragment locally and form a dense nuclear cluster of stars that undergo runaway collisions and build up a single massive star that later collapses (Whalen et al. 2008; Devecchi & Volonteri 2009). The BH would reach $10^3 - 10^4 M_\odot$ before the first SNe in the cluster would begin to disrupt it. Furthermore, some Pop III stars forming in less massive halos by H_2 cooling could reach masses as high as $10^3 M_\odot$ (Hirano et al. 2015). Both processes could lead to low-luminosity quasars at high

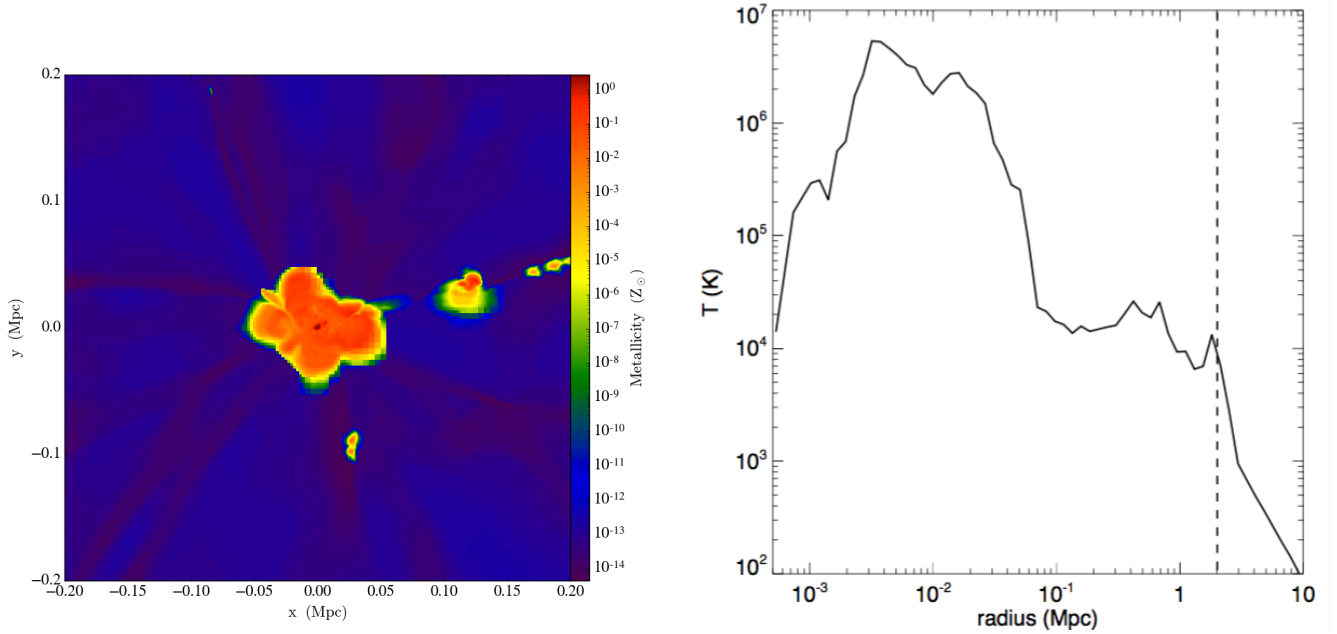


FIG. 5.— Left: metallicity slice through the center of the host galaxy of the quasar at $z = 7.1$. Distance scales are in comoving Mpc. Right: Spherically averaged temperature profile of the H II region of the quasar at $z = 7.1$. The vertical line marks the approximate boundary of gas at $> 10^4$ K at ~ 2 Mpc, the observed radius of the ionized near zone of ULAS J1120+0641.

redshift whose contribution to early reionization could be important, and their evolution in cold flows will be examined in future studies.

Quasars like J1120+0641 could be detected at even earlier epochs in the near infrared by *Euclid* and the Wide-Field Infrared Survey Telescope (WFIRST), which may be best suited to finding AGNe at $5 < z < 15$ because of their wide fields. They could then be studied with spectroscopy with *JWST* or 30 - 40 m telescopes on the ground to distinguish them from imposters such as Galactic brown dwarfs. The proximity zones of high- z quasars may also be visible at 21 cm to the Low-Frequency Array (LOFAR) and the Square Kilometer Array (SKA). Outflows from the host galaxies of such quasars and their bright centermost regions may soon be imaged by ALMA (e.g. Venemans et al. 2017).

The cosmic microwave background (CMB) could mute radio emission from the lobes of early quasars if the energy density of the CMB exceeds that of the magnetic field of the jet because relativistic electrons would preferentially cool by upscattering CMB photons rather than by synchrotron emission (Ghisellini et al. 2014). But radio flux from the jet itself could be observed by the SKA and the Extended Very Large Array (eVLA) if it is

aligned along our line of sight. X-rays from the quasar may also be detected by future high-energy missions such as the Advanced Telescope for High Energy Astrophysics (Athena). Panchromatic observations could reveal the birth and evolution of the first quasars in the universe in the decade to come.

The authors thank Britton Smith, Marta Volonteri, John Wise and Hao Xu for valuable discussions. J. S., J. L. J. and H. L. are supported by a LANL LDRD Exploratory Research Grant 20170317ER. J. W. was supported by the European Research Council under the European Community's Seventh Framework Programme (FP7/2007 - 2013) via the ERC Advanced Grant "STARLIGHT: Formation of the First Stars" (project number 339177). Work at LANL was done under the auspices of the National Nuclear Security Administration of the U.S. Department of Energy at Los Alamos National Laboratory under Contract No. DE-AC52-06NA25396. All Enzo models were performed under Institutional Computing (IC) allocations on Turquoise network platforms at LANL (Wolf).

REFERENCES

- Agarwal, B., Khochfar, S., Johnson, J. L., Neistein, E., Dalla Vecchia, C., & Livio, M. 2012, *MNRAS*, 425, 2854
- Agarwal, B., et al. 2016, *MNRAS*, 460, 4003
- Alvarez, M. A., Wise, J. H., & Abel, T. 2009, *ApJ*, 701, L133
- Aykutalp, A., Wise, J. H., Spaans, M., & Meijerink, R. 2014, *ApJ*, 797, 139
- Barnett, R., et al. 2015, *A&A*, 575, A31
- Becerra, F., Greif, T. H., Springel, V., & Hernquist, L. E. 2015, *MNRAS*, 446, 2380
- Becerra, F., et al. 2017, *MNRAS*, submitted (arXiv:1702.03941)
- Begelman, M. C. 2010, *MNRAS*, 402, 673
- Bournaud, F., Dekel, A., Teyssier, R., Cacciato, M., Daddi, E., Juneau, S., & Shankar, F. 2011, *ApJ*, 741, L33
- Bryan, G. L., et al. 2014, *ApJS*, 211, 19
- Cen, R., & Ostriker, J. P. 1992, *ApJ*, 399, L113
- Chen, K.-J., et al. 2014, *ApJ*, 790, 162
- Ciotti, L., Ostriker, J. P., & Proga, D. 2009, *ApJ*, 699, 89
- Costa, T., Sijacki, D., Trenti, M., & Haehnelt, M. G. 2014, *MNRAS*, 439, 2146
- DeBuhr, J., Quataert, E., Ma, C.-P., & Hopkins, P. 2010, *MNRAS*, 406, L55
- Dekel, A., et al. 2009, *Nature*, 457, 451
- Devecchi, B., & Volonteri, M. 2009, *ApJ*, 694, 302

- Di Matteo, T., Khandai, N., DeGraf, C., Feng, Y., Croft, R. A. C., Lopez, J., & Springel, V. 2012, *ApJ*, 745, L29
- Dijkstra, M., Ferrara, A., & Mesinger, A. 2014, *MNRAS*, 442, 2036
- Dunlop, J. S. 2013, in *Astrophysics and Space Science Library*, Vol. 396, *The First Galaxies*, ed. T. Wiklind, B. Mobasher, & V. Bromm, 223
- Feng, Y., Di Matteo, T., Croft, R., & Khandai, N. 2014, *MNRAS*, 440, 1865
- Ghisellini, G., Celotti, A., Tavecchio, F., Haardt, F., & Sbarbato, T. 2014, *MNRAS*, 438, 2694
- Glover, S. C. O., & Jappsen, A.-K. 2007, *ApJ*, 666, 1
- Hahn, O., & Abel, T. 2011, *MNRAS*, 415, 2101
- Hammerlé, L., Klessen, R., Whalen, D., Woods, T. E., & Heger, A. 2017, *MNRAS*, in prep
- Hartwig, T., et al. 2016, *MNRAS*, 462, 2184
- Hirano, S., Hosokawa, T., Yoshida, N., Omukai, K., & Yorke, H. W. 2015, *MNRAS*, 448, 568
- Hirschmann, M., Dolag, K., Saro, A., Bachmann, L., Borgani, S., & Burkert, A. 2014, *MNRAS*, 442, 2304
- Hosokawa, T., et al. 2013, *ApJ*, 778, 178
- Inayoshi, K., & Omukai, K. 2012, *MNRAS*, 422, 2539
- Inayoshi, K., Visbal, E., & Kashiyama, K. 2015, *MNRAS*, 453, 1692
- Johnson, J. L., Whalen, D. J., Fryer, C. L., & Li, H. 2012, *ApJ*, 750, 66
- Johnson, J. L., Whalen, D. J., Li, H., & Holz, D. E. 2013, *ApJ*, 771, 116
- Kitayama, T., Yoshida, N., Susa, H., Umemura, M. 2004, *ApJ*, 613, 631
- Latif, M. A., Schleicher, D. R. G., Schmidt, W., & Niemeyer, J. 2013, *MNRAS*, 430, 588
- Latif, M. A., et al. 2013b, *MNRAS*, 436, 2989
- Merloni, A., & Heinz, S. 2008, *MNRAS*, 388, 1011
- Mortlock, D. J., et al. 2011, *Nature*, 474, 616
- Pacucci, F., Volonteri, M., Ferrara, A. 2015, *MNRAS*, 452, 1922
- Park, K., & Ricotti, M. 2011, *ApJ*, 739, 2
- Pezzulli, E., Valiante, R., & Schneider, R. 2016, *MNRAS*, 458, 3047
- Planck Collaboration et al. 2016, *A&A*, 594, A13
- Regan, J. A., & Haehnelt, M. G. 2009, *MNRAS*, 396, 343
- Sakurai, Y., Inayoshi, K., & Haiman, Z. 2016, *MNRAS*, 461, 4496
- Sakurai, Y., et al. 2016b, *MNRAS*, 459, 1137
- Schleicher, D. R. G., Palla, F., Ferrara, A., Galli, D., Latif, M. 2013, *A&A*, 558, 59
- Shang, C., Bryan, G. L., & Haiman, Z. 2010, *MNRAS*, 402, 1249
- Smith, A., Bromm, V., Loeb, A. 2016, *MNRAS*, 460, 3143
- Sobral, D., Matthee, J., Darvish, B., Schaerer, D., Mobasher, B., Röttgering, H. J. A., Santos, S., & Hemmati, S. 2015, *ApJ*, 808, 139
- Sutherland, R. S., & Dopita, M. A. 1993, *ApJS*, 88, 253
- Trenti, M., Santos, M. R., & Stiavelli, M. 2008, *ApJ*, 687, 1
- Umeda, H., et al. 2016, *ApJ*, 830, L34
- Venemans, B., et al. 2017, *arXiv:1702.03852*
- Volonteri, M., Silk, J., & Dubus, G. 2015, *ApJ*, 804, 148
- Whalen, D., Abel, T., & Norman, M. L. 2004, *ApJ*, 610, 14
- Whalen, D., Meiksin, A., Hartwig, T., Bacon, D. A., & Latif, M. A. 2017, *ApJ*, in prep
- Whalen, D., van Veelen, B., O'Shea, B. W., & Norman, M. L. 2008, *ApJ*, 682, 49
- Whalen, D. J., & Fryer, C. L. 2012, *ApJ*, 756, L19
- Wise, J. H., & Abel, T. 2011, *MNRAS*, 414, 3458
- Wise, J. H., Turk, M. J., & Abel, T. 2008, *ApJ*, 682, 745
- Woods, T. E., Heger, A., Whalen, D., Hammerlé, L., & Klessen, R. 2017, *ApJ*, in prep
- Wu, X.-B., et al. 2015, *Nature*, 518, 512